JPET Fast Forward. Published on October 27, 2021 as DOI: 10.1124/jpet.121.000785
This article has not been copyedited and formatted. The final version may differ from this version.

A putative new melatonin binding site in sheep brain, MTx: preliminary observations and characteristics

Preety Shabajee-Alibay, Anne Bonnaud, Benoît Malpaux, Philippe Delagrange, Valérie Audinot, Saïd Yous, Jean A. Boutin[,1], Jean-Philippe Stephan[§], Jérôme Leprince[§], Céline Legros[2,§]

Institut de Recherches SERVIER, Croissy-sur-Seine, France (PSA, AB, PD, JAB, JPS, CL) ; Normandie Université, UNIROUEN, INSERM 1239, Laboratoire de Différenciation et Communication Neuronale et Neuroendocrine, Rouen, France (PSA, JL); INRA Val de Loire, UMR Physiologie de la Reproduction et des Comportements, Nouzilly, France (BM); Institut de Recherches Internationales SERVIER, Suresnes, France (VA); Univ. Lille, INSERM, CHU Lille, UMR-S 1172-LiNC-Lille Neuroscience & Cognition, Lille, France. (SY).

[§]These authors equally contributed to this work

JPET Fast Forward. Published on October 27, 2021 as DOI: 10.1124/jpet.121.000785
This article has not been copyedited and formatted. The final version may differ from this version.

Running Title: Characterization of a new putative melatonin binding site

Corresponding author: Jean A. Boutin, PhD : ja.boutin.pro@gmail.com

Present address: PHARMADEV (Pharmacochimie et biologie pour le développement), Faculté de Pharmacie, Toulouse, France.

Statistics:

Number of text pages, 20.

number of tables, 4

number of figures, 9

number of references, 50

number of words in the Abstract, 226

number of words in the Introduction, 681

number of words in the Discussion, 1425

Non-standard abbreviations:

4P-PDOT, 4-phenyl-2-propionamidotetraline.

CSF, cerebrospinal fluid.

DOI, 1-(2,5-dimethoxy-4-iodophenyl)-aminopropane.

GPCR, G-protein coupled receptor.

Ket, ketanserine.

MCA-NAT, 5-methoxy-carbonylamino-*N*-acetyltryptamine

MLT, melatonin.

NA, noradrenaline.

NAS, *N*-acetyl-serotonin.

NQO2, quinone reductase 2.

oMT$_1$, ovine MT$_1$ receptor.

oMT$_2$, ovine MT$_2$ receptor.

PMH, premammillary hypothalamus.

S 22153, *N*-[2-(5-ethylbenzothiophen-3-yl)ethyl]acetamide.

S 27128, 2-iodo-6-nitro-melatonin.

S 70643, *N*-[2-(6-methoxy-4-isoquinolyl)ethyl]acetamide, hydrogen chloride.

S 73229, *N*-[2-(5-methoxy-2-oxo-indolin-3(RS)-yl)ethyl]acetamide.

SD 1671, *N*-[3-(2-amino-5-methoxy-phenyl)-3-oxo-propyl]acetamide.

SD 1882, 4-iodo-melatonin.

SD 1918, 7-iodo-melatonin.

Section: Cellular and Molecular

Keywords: melatonin, pharmacology, binding site, hypothalamus, 2-[^{125}I]-melatonin, GPCR, brain, sheep.

JPET Fast Forward. Published on October 27, 2021 as DOI: 10.1124/jpet.121.000785
This article has not been copyedited and formatted. The final version may differ from this version.

Abstract

In mammals, MT_1 and MT_2 melatonin receptors are high affinity G protein-coupled receptors and are thought to be involved in the integration of the melatonin signaling throughout the brain and periphery. In the present study, we describe a new melatonin binding site, named MTx, with a peculiar pharmacological profile. This site had a low affinity for 2-[^{125}I]-melatonin in saturation assays in hypothalamus and retina (pK_D = 9.13 ± 0.05, Bmax = 1.12 ± 0.11 fmol/mg protein and pK_D = 8.81 ± 0.50, Bmax = 7.65 ± 2.64 fmol/mg protein, respectively) and a very high affinity, in competition assays, for melatonin (pKi = 13.08 ± 0.18), and other endogenous compounds. Using autoradiography, we showed a preferential localization of the MTx in periventricular areas of the sheep brain, with a density 3 to 8 times higher than those observed for ovine MT_1. In addition, using a set of well-characterized ligands, we showed that this site did not correspond to any of the following receptors: MT_1, MT_2, *MT_3*, D_1, D_2, noradrenergic, nor 5-HT_2. Based on its affinity for melatonin, MTx did not seem to be implicated in the integration of cerebral melatonin concentration variations since they were saturating for MTx. Nevertheless, it remained of prime importance because of its periventricular distribution, in close contact with the CSF, and its peculiar pharmacological profile responding to both melatoninergic and serotoninergic compounds.

Significance Statement

Herein a putative new melatonin binding site is described in sheep brain parts in close contact with the 3rd ventricle. The characteristics of the pharmacological profile of this site is different from anything previously reported in the literature. The present work forms the basis of future full pharmacological characterization.

JPET Fast Forward. Published on October 27, 2021 as DOI: 10.1124/jpet.121.000785
This article has not been copyedited and formatted. The final version may differ from this version.

1 Introduction

The hormone melatonin (MLT) is mainly secreted in the bloodstream by the pineal gland and is implicated in many physiological functions including biological rhythms, reproduction, neuroprotection, immunity, and synchronization of circannual rhythms (Arendt, 1995; Pandi-Perumal et al., 2006). In mammals, three MLT binding sites were described: two of them, MT_1 and MT_2, are G protein-coupled receptors (GPCR), (Reppert et al., 1994; Reppert et al., 1995) whereas the third one, MT3, a poor affinity binding site (Duncan et al., 1986) has been identified as the cytoplasmic quinone reductase 2 (NQO2) (Nosjean et al., 2000; Nosjean et al., 2001; Boutin and Ferry, 2019). MLT has been recently described as potentially having about a dozen more protein targets (Liu et al., 2019), most of which are poorly described and/or characterized (Boutin and Jockers, 2020), beside the classical membrane receptors and NQO_2.

Molecular cloning of MT_1 and MT_2 receptors has revealed a high homology degree among species (Reppert et al., 1994; Reppert et al., 1995), with a similar sub-nanomolar affinity for MLT (Dubocovich, 1995). Extended pharmacological studies on MT_1 and MT_2 receptors have led to the discovery of some ligands more specific for one or the other subtype (Audinot et al., 2003; Legros et al., 2013; Legros et al., 2014b), although the chemical landscape of MLT ligands is still rather scarce (Boutin et al., 2020). Both receptors have been now crystallized, leading to new knowledge in the orientations of the molecules in their receptors (Johansson et al., 2019; Stauch et al., 2019).

Most species, including rat (Audinot et al., 2008), mouse (Devavry et al., 2012) or human (Audinot et al., 2003) express the two MLT receptors. In sheep, the MT_2 mRNA is particularly abundant in the retina, the *pars tuberalis*, the mammillary bodies and the choroid plexus, while it is poorly expressed in the premammillary hypothalamus (PMH), the caudate nucleus and the pineal gland (Cogé et al., 2009). PMH was also identified as a target tissue for a physiological action of MLT (Malpaux et al., 1998). In this

JPET Fast Forward. Published on October 27, 2021 as DOI: 10.1124/jpet.121.000785
This article has not been copyedited and formatted. The final version may differ from this version.

cerebral area, MLT controls reproductive seasonality in sheep and 2-[^{125}I]-MLT binding sites sustain one order of magnitude higher density than in any other hypothalamic regions (2 fmol/mg protein vs. 0.2-0.4 fmol/mg protein) (Malpaux et al., 1998), although this density is much lower than those observed in the *pars tuberalis* (Piketty and Pelletier, 1993; Malpaux et al., 1998). These binding sites were identified as the oMT$_1$ receptor (Mailliet et al., 2004)(Migaud et al., 2005). PMH and other periventricular areas expressing high affinity MLT receptors are exposed to high concentrations of MLT because of their exposition to the cerebrospinal fluid (CSF) of the third ventricle (Malpaux et al., 1998) and of the diffusion of MLT from this compartment (Legros et al., 2014a). The MLT concentrations observed in these areas can be as elevated as 4100 pg/ml (17.7 nM) whereas they are around 84 pg/ml (0.4 nM) in more distal areas from the ventricle (Legros et al., 2014a). These MLT concentrations in the nanomolar range are saturating for MT$_1$ or MT$_2$ receptors both during the night and the day and thus are not consistent with the alternation of high and low concentrations, which is critical for the integration of the cerebral melatoninergic signal.

This particular feature led us to hypothesize that another MLT binding site, critical for the integration of the day/night alternation in the presence of MLT, might be expressed in the ovine brain.

To test this hypothesis, we performed a pharmacological characterization of MLT binding sites present in the sheep hypothalamus. To characterize the hypothalamic distribution and the identity of MLT binding sites, two types of experiments were performed: autoradiography with 2-[^{125}I]-MLT on hypothalamic sections and pharmacological profile on hypothalamus membrane preparations. These observations led to evidence that a new MLT binding site exists in sheep brain that we named MTx. This binding site has several features dramatically different from the previously described MLT binding sites (MT$_1$, MT$_2$, Mel1c, NQO2). Further work will be necessary to lay the molecular basis of this new protein, not necessarily a GPCR, to better understand its role in integrating MLT signaling pathways.

JPET Fast Forward. Published on October 27, 2021 as DOI: 10.1124/jpet.121.000785
This article has not been copyedited and formatted. The final version may differ from this version.

2 Materials & Methods

2.1 Reagents and ligands

2-[^{125}I]-MLT (specific activity: 2000 Ci/mmol) was purchased from Amersham Pharmacia Biotech (USA). MLT, 2-I-MLT, N-acetyl-serotonin (NAS), serotonin (5-HT), 1-(2,5-dimethoxy-4-iodophenyl)-aminopropane (DOI), and dopamine (DA) were obtained from Sigma-Aldrich (France). 5-Methoxy-carbonylamino-N-acetyltryptamine (MCA-NAT) and 4-phenyl-2-propionamidotetraline (4P-PDOT) were obtained from Tocris (UK), ketanserine (Ket) and noradrenaline (NA) were obtained from Sigma-Aldrich.

Eleven synthetic analogues of MLT were used: 2-I-MLT, S 22153, 4P-PDOT, SD 1882, SD 1918, S 27128, S 22958, S 73229, S 70643, NAS and SD 1671 (**Figure 1**). The following ones belong to the MLT compound library of Les Laboratoires Servier. Their respective syntheses were previously reported as indicated in the following list: S 22153 (*N*-[2-(5-ethylbenzothiophen-3-yl)ethyl]acetamide) (Legros et al., 2020); SD 1882 (4-iodo-melatonin) (Legros et al., 2020); SD 1918 (7-iodo-melatonin) (Legros et al., 2014b); S 27128, 2-iodo-6-nitro-melatonin (Leclerc et al., 2002); S 22958 (4-(8-chloro-7-methoxy-1-naphthyl)-*N*-ethyl-butanamide) (Leclerc et al., 1998); S 73229 (*N*-[2-(5-methoxy-2-oxo-indolin-3(RS)-yl)ethyl]acetamide, racemate) (Lozinskaya et al., 2011); S 70643, (*N*-[2-(6-methoxy-4-isoquinolyl)ethyl]acetamide, hydrogen chloride) (Ettaoussi et al., 2021); SD 1671,(*N*-[3-(2-amino-5-methoxy-phenyl)-3-oxo-propyl]acetamide) (Harthé et al., 2003). All compounds were dissolved in DMSO at a stock concentration of 10 mM and stored at -20°C.

JPET Fast Forward. Published on October 27, 2021 as DOI: 10.1124/jpet.121.000785
This article has not been copyedited and formatted. The final version may differ from this version.

2.2 **Hypothalamus, *pars tuberalis* and retina tissues**

Lambs obtained from the SODEM slaughterhouse (Le Vigeant, France) were euthanized in the morning (07:00 to 12:00) between January and June. Brains were removed from the skull and frozen in isopentane maintained at -50°C with liquid nitrogen after collecting the *pars tuberalis* that were separately frozen in liquid nitrogen vapors. Retinas were dissected from the lamb orbits, by reversing the membranes inside out and scraping the retina surface. Hypothalamus, *pars tuberalis* and retina were stored at -80°C. The delay between the slaughter and freezing of collected samples did not excess 10 min.

Brains were dissected at 4°C to isolate the hypothalamic area defined by autoradiography (data not shown) and used for the membrane preparations (**Scheme 1**), brain block 3 mm-thick on the rostro-caudal axis and centered on the PMH, limited ventrally by the basis of the brain and dorsally by the floor of the lateral ventricles, 3 mm wide on either side of the third ventricle, no tissue from the *pars tuberalis* was present in the samples.

2.3 **Autoradiography**

Experiments were conducted on 2 adult sheep males, sacrificed by decapitation (within 2 h after lights-on). Brains were quickly removed and frozen in isopentane maintained at -50°C with liquid nitrogen. Frozen frontal brain sections (15 µm) were generated by microtome-cryostat (Leitz Cryostat 1720, Saint-Julie, QC, Canada) at -20°C. Sections were collected on 3-amino-propyl-ethoxy-silane gel coated slides (Sigma-Aldrich) and returned at -80°C until use. Analysis was performed on sections in the posterior part of the hypothalamus, centered on the PMH. All procedures were approved by the French Ministry of Agriculture and performed by authorized investigators (authorization n° A37802). To saturate the binding sites with 2-[^{125}I]-MLT, sections were washed with PBS buffer (0.01 M, 0.1 M NaH_2PO_4, 154 mM NaCl, pH 7.4) at 4°C, incubated for 1 h at room temperature with 100 µl of PBS containing 2-[^{125}I]-MLT 14 to 14250 pM (specific activity of 2000 Ci/mmol), rinsed twice at 4°C with PBS (2 and 3 min), fixed with 4% paraformaldehyde at 4°C for 10 min and dipped in water for 10 min. Adjacent sections were incubated with

JPET Fast Forward. Published on October 27, 2021 as DOI: 10.1124/jpet.121.000785
This article has not been copyedited and formatted. The final version may differ from this version.

MLT 10 µM to assess non-specific binding as previously described (Malpaux et al., 1998). Autoradiograms were generated with air-dried sections placed in X-ray cassettes with hyperfilm Biomax MR (Amersham, France). [^{125}I] microscale standards were generated with 7 doses of 2-[^{125}I]-MLT in pure ethanol dispersed on thin layer chromatography silicate gel (Macherey-Nagel, France). Exposure time was 1 day for high concentrations (730-14250 pM) and 14 days for lower concentrations (14-5300 pM), at room temperature. Binding intensity was assessed by an image analysis system (Biocom Histo 500, Amersham, France). After non-specific signal subtraction, mean grey density was transformed in cpm using the microscale standards and data were converted to fmol/mg protein as described previously (Legros et al., 2014a). MLT binding site density was assayed in 5 different areas of the posterior hypothalamus: the sub-fornical area of the PMH, the areas bordering the third and the lateral ventricles, the mammillothalamic tract region and the region between the third ventricle and the lateral ventricles. The binding on the *pars tuberalis* was used as control for oMT$_1$ receptor binding.

2.4 **Membrane preparations**

A total of 1125 brains and about 200 retinas were collected from undetermined gender and age sheep in Sept/Jan/June/April between 6 am-11 am, in the SODEM meat slaughterhouse. Cerebral structures and retinas were crushed and homogenized with an Ultra-turrax (Janke-Kunkel, Imlab, Belgium) in grinding buffer (5 mM Tris/HCl, 2 mM EDTA, pH 7.4, 4°C). Homogenates were then centrifuged (1000 g, 12 min, 4°C) and the supernatants were ultra-centrifuged (10 000 g, 35 min, 4°C). Pellets were suspended in conservation buffer (50 mM Tris/HCl, 6 mM ascorbic acid, 4 mM $CaCl_2$, 4% glycerol, pH 7.4). Protein quantification was performed according to Biorad Kit instructions (Biorad SA, France). Membrane preparations were homogenized with Kinematica polytron and aliquots at 5 mg protein/ml were stored at -80°C until use. Seventeen membrane preparations were performed from the 1125 above mentioned brains. They were all characterized by Scatchard/saturation experiments and under our experimental conditions, a clear two binding sites profile was identified.

2.5 **2-[^{125}I]-MLT binding assay**

JPET Fast Forward. Published on October 27, 2021 as DOI: 10.1124/jpet.121.000785
This article has not been copyedited and formatted. The final version may differ from this version.

Membranes and ligands were diluted in binding buffer (50 mM Tris/HCl, 6 mM ascorbic acid, 4 mM $CaCl_2$, pH 7.4) and incubated for 4 h at room temperature under permanent agitation and sheltered from light. Proteins were diluted for a final volume of 500 µl at the concentration of 1 mg/ml. In saturation assays, 2-[^{125}I]-MLT was used with concentrations ranging from 1 pM to 2-2.5 nM. In competition assays, 2-[^{125}I]-MLT was maintained at 35 pM for oMT1 binding and 350 pM for MTx binding and compounds were used in the range of 10 fM-1 µM. For the experiments performed in presence of MLT analogues SD 1882 and S 27128, compounds were diluted at the final concentration of 1 pM, for both saturation and competition experiments, and S 22153 at the final concentration of 1 µM, for competition experiment only. Non-specific binding was determined with 0.1 µM of cold 2-I-MLT. Reaction was stopped by ultrafiltration with Filtermate harvester or with Brandel through Whatman GF/B filters, followed by three successive washes with ice-cold binding buffer.

2.6 **Data analysis**

Data were analyzed by using the program PRISM (GraphPad Software Inc., California, USA). For saturation experiments, the maximal concentration of binding site (Bmax) and the dissociation constant of the radioligand (K_D) values were calculated according to the Scatchard method. For competition experiments, because of the high risk of ligand depletion, and to take into account not only the radioligand concentration but also the receptor concentration inhibition constants (Ki) were calculated according to (Jacobs et al., 1975) and described in Zhen et al. (2010).

$$IC50 = Ki + \frac{Ki}{KD}([Lt] + [Rt] - \frac{3}{2}[LRmax])$$

In which [Lt] is the total concentration of radioligand, [Rt] the total concentration of receptor and [LRmax], the concentration of receptor-radioligand complex. Relevant statistical models for saturation and competition, one or two sites, were used (extra sum-of-squares F-test).

2.7 **Nomenclature of targets and ligands**

All targets and ligands used throughout this manuscript conform with the guidelines outlined by the International Union of Basic and Clinical Pharmacology and British Pharmacological Society

JPET Fast Forward. Published on October 27, 2021 as DOI: 10.1124/jpet.121.000785
This article has not been copyedited and formatted. The final version may differ from this version.

(IUPHAR/BPS) Guide to Pharmacology (Alexander et al., 2019). Furthermore, the recommendation for the description of new MLT targets have been followed (Cecon et al., 2020).

JPET Fast Forward. Published on October 27, 2021 as DOI: 10.1124/jpet.121.000785
This article has not been copyedited and formatted. The final version may differ from this version.

3 Results

3.1 Autoradiographic observations

In autoradiographic experiments conducted on sheep brain slices (**Figure 2**), we noticed that the density of specific binding sites increased with the concentration of 2-[^{125}I]-MLT up to 272 pM in the *pars tuberalis* in line with previous observations (deReviers et al., 1989; Morgan et al., 1989; Bittman and Weaver, 1990; Stankov et al., 1991). Typical autoradiograms clearly show the existence of MLT binding sites in the areas around the sub-fornical and the 3rd ventricle regions, after 14 days exposure (**Figure 2**). The specificity of the binding site is obvious, as the non-specific experiments did not show any matching density in the same regions, excluding the possibility of an artefact due to our experimental conditions.

3.2 Binding in *pars tuberalis*

The density of MLT binding site was close to 60 fmol/mg protein (**Figure 3A**) and no further increase was observed at higher concentrations of 2-[^{125}I]-MLT. Furthermore, in *pars tuberalis* membrane preparations, saturation tests revealed only one binding site (**Figure 3B**), with K_D equal to 13.9 ± 2.5 pM and Bmax equal to 39.5 ± 8.0 fmol/mg protein (**Table 1**), both results perfectly match the binding characteristics of the oMT_1 (Cogé et al., 2009) and oMT_2 receptors from *pars tuberalis* (Mailliet et al., 2004).

3.3 Binding in posterior hypothalamus

The next steps were intended to scrutinize, under similar conditions to the ones described above in *pars tuberalis*, slices of the subregional hypothalamus. In the five hypothalamic areas studied (**Scheme 1 and Figure 4**), namely the border of the lateral ventricle, the region between the third and the lateral ventricles, that are the mammillothalamic tract, the subfornical part of the PMH and the border of the third ventricle, one can observe a first plateau for 2-[^{125}I]-MLT concentrations ranging between 270 and 3200 pM corresponding to a level of 1.8 fmol/mg protein, followed by an increase in binding between 5300 and

JPET Fast Forward. Published on October 27, 2021 as DOI: 10.1124/jpet.121.000785
This article has not been copyedited and formatted. The final version may differ from this version.

11500 pM and a second plateau (**Figure 4**). The highest density of MLT binding sites (> 10 fmol/mg protein) corresponding to this second plateau was observed in a region close to the lateral ventricles (**Figure 4**).

As shown in **Figure 5**, the saturation experiments performed on hypothalamic membranes (n = 17, from 11 different membrane preparations) using 2-[^{125}I]-MLT, revealed two binding sites (F test) in those preparations **(Table 1**): a high affinity binding site (pK_D = 10.58 ± 0.07) corresponding to oMT_1 and a second one with a "poorer" affinity (pK_D = 9.13 ± 0.05) that we named MTx for the sake of simplicity in the present work. The density of these MLT binding sites were 0.40 ± 0.05 fmol/mg protein for the oMT_1 binding site and 1.12 ± 0.11 fmol/mg protein for MTx. We identified the first binding site as oMT_1 or oMT_2 based on both their previously reported characteristics (Mailliet et al., 2004; Cogé et al., 2009) and the present observations.

In brief, the net results of these two first sets of experiments were that, in similar experimental conditions not fundamentally different from standard MLT binding protocols, we showed the existence of an extra binding site in a part of the hypothalamus in close vicinity of the CSF. Under our experimental conditions, as mentioned above, the signal-to-noise ratio was in the 30% range.

3.4 **Pharmacological profile of *pars tuberalis* and hypothalamic binding sites**

In order to further characterize those binding sites, we performed competition assays in the presence of 2-[^{125}I]-MLT in *pars tuberalis* (data not shown) and in hypothalamic membranes, following the recommendations for new MLT binding sites (Cecon et al., 2020). To segregate between both sites in hypothalamus, we used different saturating concentrations of 2-[^{125}I]-MLT: 35 pM for oMT_1/oMT_2 and 350 pM for the putative MTx new binding site. **Figure 6** reports the results of these competition assays performed on those membranes.

At the 35 pM concentration of 2-[^{125}I]-MLT, the competition assays between 2-[^{125}I]-MLT and MLT or 2-I-MLT revealed only one binding site with the following characteristics on *pars tuberalis* membranes: pKi of 10.38 ± 0.08 for MLT (n = 3); pKi of 10.46 ± 0.04 pM for 2-I-MLT (n = 15) (data not shown) while the

JPET Fast Forward. Published on October 27, 2021 as DOI: 10.1124/jpet.121.000785
This article has not been copyedited and formatted. The final version may differ from this version.

following characteristics were recorded from hypothalamic membranes: pKi of 9.76 ± 0.07 for MLT (n = 5), and pKi of 10.41 ± 0.06 for 2-I-MLT (n = 18) (**Figure 6 and Table 2**). To compare these data with those from oMT_1 and oMT_2, we investigated the behavior of 16 other compounds (**Figure 1**), coming from the standard characterization of our cloned MLT receptors as reported in recent years for human MLT receptors (Audinot et al., 2003), rat MLT receptors (Audinot et al., 2008), mouse MLT receptors (Devavry et al., 2012), sheep MLT receptors (Cogé et al., 2009) and hamster MLT receptor (Gautier et al., 2018), as well as some compounds from the general safety pharmacology profile. Under our experimental protocol, only MCA-NAT, 5-HT, Ket, DOI, DA and NA did not compete with the tracer (n = 2 for *pars tuberalis* membranes and n = 4 for hypothalamus membranes). All the other compounds showed monophasic curves (**Figure 6 and Table 2**). Of note, the binding site characteristics do not fit any of the DA, or NA receptors, and would fit more closely an MLT-type profile, essentially due to the displacement of MLT itself.

As shown on the **Figure 6**, competition experiments at higher concentration of 2-[^{125}I]-MLT (350 pM) were performed on hypothalamic membranes. Notably, biphasic curves were recorded for MLT and 2-I-MLT (F test), with a high affinity binding site (pKi = 9.77 ± 0.11, n = 10, and pKi = 10.61 ± 0.09, n = 31, for MLT and 2-I-MLT, respectively) and a very high affinity binding site (pKi = 13.08 ± 0.18, n = 10, and pKi = 13.24 ± 0.14, n = 31, for MLT and 2-I-MLT, respectively), as shown in **Table 2**.

Table 2 summarizes all the binding data obtained for the 18 compounds on *pars tuberalis* for the oMT_1/oMT_2 receptors at 35 pM 2-[^{125}I]-MLT and for the hypothalamic oMT1/oMT2 and MTx receptors at 35 and 350 pM of 2-[^{125}I]-MLT. In competition assays, 4P-PDOT, SD 1882, SD 1918, S 27128, S 22958, and S 70643 exhibited curves at 350 pM of 2-[^{125}I]-MLT (n = 4 per ligand) that were best fitted by a two rather than a single site analysis (F test) corresponding to a high and very high affinity binding sites, respectively (**Figure 6 and Table 2**). In contrast, MCA-NAT, DOI, Ket, DA and NA did not show any affinity on hypothalamic membranes while S 22153, S 73229, 5-HT, NAS and SD 1671 displayed only one-site curve on these membrane preparations (oMT1 for S 22153; MTx for S 73229, 5-HT, NAS and SD 1671) (**Figure 6 and Table 2**). Comparison of MLT pKi's on hypothalamic oMT1/oMT2 obtained with 35 pM 2-[^{125}I]-MLT with those obtained with a higher concentration of 2-[^{125}I]-MLT indicated that (i) 4P-PDOT, SD 1882, SD 1918, S 27128, S 22958 and S 70643 competed with MTx as well as with oMT1 and

JPET Fast Forward. Published on October 27, 2021 as DOI: 10.1124/jpet.121.000785
This article has not been copyedited and formatted. The final version may differ from this version.

oMT2 expressed in the hypothalamus; and (ii) 5-HT bound only on MTx whereas S 22153 only bound on oMT1/oMT2 (**Table 2**). Among all the compounds tested, SD 1882 and S 27128 appeared to be more discriminatory for the two binding sites, with 4 to 5 order of magnitude shifts between the Ki's at the MTx binding sites and the oMT1/oMT2 canonical receptors (**Table 2)**. S 22153 is deprived of any affinity for MTx, thus representing a specific compound for the oMT1/oMT2 site (**Figure 6 and Table 2**).

3.5 **MTx presents an atypical pharmacological profile.**

By comparting the Scatchard plots in figure 7D (*pars tuberalis* membranes) and 7A (hypothalamus membranes), one can notice that the first is mono-site (Figure 7D), while the second shows two sites (Figure 7A). Hypothalamus, is thus a tissue in which MTx is not detected. The site in hypothalamus clearly corresponds to oMT, while in *pars tuberalis*, both oMTs and MTx can be detected. Because SD 1882 or of S 27128 showed specificity at MTx over oMT_1/oMT_2, we believed they could be useful tools to segregate between those receptor and binding site. To address this hypothesis, we added 1 pM of either compounds in saturation assays. These additions induced monophasic curves on hypothalamic membranes, with a pK_D of 10.49 ± 0.20 and a Bmax of 0.59 ± 0.15 fmol/mg protein for SD 1882 and a pK_D of 10.51 ± 0.19 and a Bmax of 0.60 ± 0.13 fmol/mg protein for S 27128 (n = 3 for each ligand) (**Figure 7 and Table 1**). This concentration SD 1882 or of S 27128 (1 pM) was sufficient to inhibit the 2-[^{125}I]-MLT binding at the very-high affinity site (MTx) but not at the oMT1 receptor. Thus, both compounds can be used as efficient competitors of this putative MTx binding site as much more as they both are iodinated compounds.

Conversely, in competition assays, S 22153 (1 µM), that showed no affinity for the MTx site, inhibited the displacement of 350 pM 2-[^{125}I]-MLT at the oMT1 receptor expressed in hypothalamic membranes by both 2-I-MLT and MLT (**Figure 8 and Table 3**). On the other hand, addition of 1 pM of SD 1882 or of S 27128 inhibited the ability of 2-I-MLT and MLT to compete with 2-[^{125}I]-MLT binding at MTx, resulting in a dose-response monophasic curve showing one binding site corresponding to oMT_1 (pKi = 10.42 ± 0.45 and pKi = 10.44 ± 0.50, respectively for 2-I-MLT and pKi = 9.80 ± 0.46 and pKi = 10.24 ± 0.79, respectively for MLT). Taken as a whole, these results indicate that these 3 compounds behaved as discriminating molecules between oMT_1 and MTx: one specific of oMT_1 (S 22153) and the two others specific of MTx (SD 1882 and S 27128).

JPET Fast Forward. Published on October 27, 2021 as DOI: 10.1124/jpet.121.000785
This article has not been copyedited and formatted. The final version may differ from this version.

3.6 **Saturation experiments on retina**

To reinforce these finding, it was necessary to check another tissue for the presence of the MTx binding site, using our similar protocol for binding. Saturation experiments on sheep retina membrane preparations with 2-[^{125}I]-MLT concentrations ranging from 0.01 to 5 nM showed two MLT binding sites (F test) with affinities similar to the ones obtained with hypothalamus membranes. The first site exhibited a high affinity binding site (pK_D = 10.18 ± 0.20), comparable to the oMT1 affinity and a second site with a lower affinity (pK_D = 8.81 ± 0.50) comparable to MTx affinity. The density of MLT binding sites was 2.47 ± 0.43 fmol/mg protein for oMT1 receptor and 7.65 ± 2.64 fmol/mg protein for the lower affinity binding site MTx (**Figure 9)**. These data suggest the presence of MTx in the retina as well, in addition to the oMT1 and oMT2 receptors (Mailliet et al., 2004; Cogé et al., 2009), at a higher density than in hypothalamus, making this organ a good candidate for target deconvolution.

JPET Fast Forward. Published on October 27, 2021 as DOI: 10.1124/jpet.121.000785
This article has not been copyedited and formatted. The final version may differ from this version.

4 Discussion

MLT exerts its multiple roles in the organism through several targets. The main proteins, reported since the early 90's, are 2 GPCRs, MT_1 and MT_2, but several others have been described: *MT3*/NQO2 (Boutin and Ferry, 2019) or hypothesized like the nuclear receptor ROR (Jan et al., 2011; Boutin, 2018). The two cloned GPCRs, show a high affinity for MLT (K_D = 20-200 pM, *i.e.* pK_D = 10.70-9.70). These receptors present similar pharmacological profiles toward melatoninergic ligands, but also have some selective ligands to differentiate from each other (Boutin et al., 2017). At pharmacological concentrations (> 1 µM), MLT also binds to other proteins that probably induce its anti-oxidative effects, like the cytoplasmic NQO2 (Calamini et al., 2008).

The tremendous number of pharmaco-therapeutic actions reported for MLT strongly points at MLT having many more targets than currently described, even though the concentrations used for those observations are so large that they might come from unspecific interaction(s) with targets or pathways (Boutin, 2016, 2018; Boutin and Jockers, 2020). In the present study, we describe a putative new MLT binding site, with a peculiar pharmacological profile, that we propose to name MTx. In sheep, this binding site was found in both hypothalamus and retina. It differs from MT_1 and MT_2, because it can bind 5-HT, unlike the classical MLT receptors. These two observations are key elements on the special nature of this MLT binding site. Furthermore, it discriminates from classical serotoninergic receptors because it binds MLT. We also identified 2 selective ligands for MTx: SD 1882 (4-iodo-MLT) and S 27128 (2-iodo-6-nitro-MLT). Binding experiments performed with melatoninergic ligands and other neurotransmitters suggest that this new binding site MTx is not a conventional MLT receptor, nor a serotoninergic, adrenergic, and dopaminergic receptor (**Table 4**).

We made different hypotheses concerning this binding site. The first interpretation is that MTx is a new MLT binding site with a very high affinity that has never been described before. The affinity difference between the saturation (nM range) and competition (pM range) experiments was surprising. Indeed, affinities were expected to be in the same range as described for the oMT1 receptor. To explain this

JPET Fast Forward. Published on October 27, 2021 as DOI: 10.1124/jpet.121.000785
This article has not been copyedited and formatted. The final version may differ from this version.

difference, we hypothesized that endogenous MLT present in the membrane might potentially be bound to the MTx site conversely to oMT1 receptor that displays a lower affinity for MLT. In order to validate this hypothesis, endogenous MLT was assayed in membrane preparations and its concentration was in the 40 fM range. In saturation assays, a high concentration of 2-[^{125}I]-MLT (> 3200 pM) is required to shift the binding of endogenous MLT on the MTx binding site, and thus this site is characterized by a higher constant of dissociation. Regarding the competition assays, a high concentration of 2-[^{125}I]-MLT (350 pM) to displace the endogenous MLT is always required to observe the MTx site. In this case, low quantities of MLT or other specific ligands (in the picomolar range) should displace 2-[^{125}I]-MLT from the MTx binding sites. To summarize, MTx displays a very high affinity for endogenous MLT, so it requires a high concentration of 2-[^{125}I]-MLT to dissociate MLT from MTx, in order to study this new binding site by autoradiography. To prove the implication of the endogenous MLT in "saturation affinity shift", different experiments could be considered: (i) increase the number of washes of membrane proteins during the membrane preparation protocol and (ii) use pinealectomized sheep to perform the experiments. However, neither of these two approaches is fully satisfactory since increasing the number of washes could reduce the density of MTx binding sites and could result in the loss of a large part of the specific signal. The use of pinealectomized sheep requires a difficult surgery and a large number of animals to prepare the membranes (1 brain for 1 to 4 points in binding assays). Moreover, the absence of MLT might influence, *in vivo*, the pharmacological parameters of the receptors and binding sites in term of density and/or sensibility.

Another hypothesis concerning this new binding site could be related to the dimerization (homo or hetero) of classical MLT receptors (Ayoub et al., 2004; Jockers et al., 2008; Kamal et al., 2015), leading to a new heterodimeric pharmacological entity. This can be excluded by the fact that specific ligands of MT_1 or MT_2 also binds dimers (Jockers et al., 2008), but not MTx (data not shown). In a recent study, Kamal et al. (2015) showed that the classical MLT receptors MT_2 could dimerize with the 5-HT_{2c} receptor. Therefore, we wondered if MTx could be this MT_2/5HT_{2c} heterodimer. We definitively rejected this hypothesis, since the MT_2-specific antagonist 4P-PDOT did not bind to MTx, while it acts on the heterodimer functionality (Kamal et al., 2015). Ultimately, one might also hypothesize that MTx is not a GPCR, but another type of receptor. To rule out a GPCR hypothesis, we attempted to perform binding in the presence of GTPNHP, but

JPET Fast Forward. Published on October 27, 2021 as DOI: 10.1124/jpet.121.000785
This article has not been copyedited and formatted. The final version may differ from this version.

the compound was without any effect possibly due to the very low expression of MTx in membranes (data not shown), or because it is not a GPCR.

We also put forward a possibility according to which, like MT3/NQO_2, MTX is not a binding site, but a catalytic site in which the association between the substrate (i.e. MLT and analogues) and the putative protein would not obey "simple" rules of Cheng & Prusoff (Cheng and Prusoff, 1973). This feature is naturally completely different than for the oMT receptor behaviors, as shown herein in the same sets of experiments. This question cannot be simply addressed by binding, but would require calorimetric approaches, as we set up for NQO_2 (*MT_3*) once it was cloned (Calamini et al., 2008). It was basically our reasoning when we attempted the purification of *MT_3*, (Nosjean et al., 2000), because the conditions of binding were so different the standard conditions reported for GPCRs. This reasoning was also enforced by the fact that the binding experiments of MTx were insensitive to GTPγS (see above), strongly suggesting that MTx was not a GPCR.

In conclusion, our data support MTx as a new MLT binding site that has never been described before. We hypothesized that this binding site is not one of the described heterodimers nor one of the other classical neurotransmitter receptors. Indeed, as we showed, using the same tissues, the same experimental set up, the same compounds, we found a part of the behavior corresponding beyond any doubt to the standard oMT receptor behavior, as reported by us and by others, while part of the observations did not obey the same pharmacological rules, pointing out either, unlikely, at an unconventional GPCR or, more probably, at a protein that is membrane associated but not a GPCR. It displays a peculiar pharmacological profile as it also binds 5-HT and NAS, and other precursors and derivatives of MLT. However, the role of MTx will not be completely elucidated until the molecular entity behind this activity is identified. Based on our data, the retina might be a tissue of interest to support such deconvolution effort. The fact that MTx is detectable and express in the retina and the existence of selective compounds for MTx, such as SD 1882 and S 27128, should facilitate the identification and the cloning of the target protein. As a reminder, it is that way we could purify MT3 (by using a derivative of the MCA-NAT relatively specific binder of *MT_3*). Both compounds (SD 1882 and S 27153) are iodinated compounds and could be used as specific binders, an

JPET Fast Forward. Published on October 27, 2021 as DOI: 10.1124/jpet.121.000785
This article has not been copyedited and formatted. The final version may differ from this version.

approach we previously described for alternative binding strategies at MLT receptors (Legros et al., 2013; Boutin et al., 2017).

Subsequently, the unfolding of the physiological function of this new binding site will shed some light on MLT actions.

Author contributions:

Participated in research design: Legros, Delagrange, Stephan, Leprince, Malpaux

Conducted experiments: Shabajee-Alibay, Bonnaud

Contributed new reagents or analytic tools: Yous

Performed data analysis: Legros, Shabajee-Alibay, Stephan, Leprince

Wrote or contributed to the writing of the manuscript: Boutin, Legros, Leprince, Delagrange, Shabajee-Alibay Audinot, Stephan

Acknowledgments: The authors wish to thank the sheep team of INRA UE-PAO for animal care; J.-P. Dubois, G. Gomot, J.-P. Petit, C. Moussu and H. Leroux for help with the experiments; SODEM Covimo, Le Vigeant, France for providing brain tissue. P. Shabajee-Alibay was supported by a PhD grant from ANRT.

Competing interests' statement: The authors declare that this article was written in the absence of any commercial or financial relationships that could be construed as a potential conflict of interest.

References

Alexander SPH, Christopoulos A, Davenport AP, Kelly E, Mathie A, Peters JA, Veale EL, Armstrong JF, Faccenda E, Harding SD, Pawson AJ, Sharman JL, Southan C, and Davies JA (2019) THE CONCISE GUIDE TO PHARMACOLOGY 2019/20: G protein-coupled receptors. *Br J Pharmacol* **176 Suppl 1:**S21-S141 doi: 10.1111/bph.14748.

Arendt J (1995) *Melatonin and the mammalian pineal gland*, 1. ed. Chapman & Hall, London, Glasgow, Weinheim et al.

Audinot V, Bonnaud A, Grandcolas L, Rodriguez M, Nagel N, Galizzi J-P, Balik A, Messager S, Hazlerigg DG, Barrett P, Delagrange P, and Boutin JA (2008) Molecular cloning and pharmacological characterization of rat melatonin MT1 and MT2 receptors. *Biochem Pharmacol* **75:**2007–2019 doi: 10.1016/j.bcp.2008.02.022.

Audinot V, Mailliet F, Lahaye-Brasseur C, Bonnaud A, Le Gall A, Amossé C, Dromaint S, Rodriguez M, Nagel N, Galizzi J-P, Malpaux B, Guillaumet G, Lesieur D, Lefoulon F, Renard P, Delagrange P, and Boutin JA (2003) New selective ligands of human cloned melatonin MT1 and MT2 receptors. *Naunyn Schmiedebergs Arch Pharmacol* **367:**553–561 doi: 10.1007/s00210-003-0751-2.

Ayoub MA, Levoye A, Delagrange P, and Jockers R (2004) Preferential formation of MT1/MT2 melatonin receptor heterodimers with distinct ligand interaction properties compared with MT2 homodimers. *Mol Pharmacol* **66:**312–321 doi: 10.1124/mol.104.000398.

Bittman EL and Weaver DR (1990) The distribution of melatonin binding sites in neuroendocrine tissues of the ewe. *Biol Reprod* **43:**986–993 doi: 10.1095/biolreprod43.6.986.

Boutin JA (2016) Quinone reductase 2 as a promising target of melatonin therapeutic actions. *Expert Opin Ther Targets* **20:**303–317 doi: 10.1517/14728222.2016.1091882.

Boutin JA (2018) *How Can Molecular Pharmacology Help Understand the Multiple Actions of Melatonin: 20 Years of Research and Trends*. IntechOpen, [sine loco].

Boutin JA, Bonnaud A, Brasseur C, Bruno O, Lepretre N, Oosting P, Coumailleau S, Delagrange P, Nosjean O, and Legros C (2017) New MT_2 Melatonin Receptor-Selective Ligands: Agonists and Partial Agonists. *Int J Mol Sci* **18** doi: 10.3390/ijms18071347.

Boutin JA and Ferry G (2019) Is There Sufficient Evidence that the Melatonin Binding Site MT3 Is Quinone Reductase 2? *J Pharmacol Exp Ther* **368:**59–65 doi: 10.1124/jpet.118.253260.

Boutin JA and Jockers R (2020) Melatonin controversies, an update. *J Pineal Res:*e12702 doi: 10.1111/jpi.12702.

Boutin JA, Witt-Enderby PA, Sotriffer C, and Zlotos DP (2020) Melatonin receptor ligands: A pharmaco-chemical perspective. *J Pineal Res* **69:**e12672 doi: 10.1111/jpi.12672.

Calamini B, Santarsiero BD, Boutin JA, and Mesecar AD (2008) Kinetic, thermodynamic and X-ray structural insights into the interaction of melatonin and analogues with quinone reductase 2. *Biochem J* **413:**81–91 doi: 10.1042/BJ20071373.

Cecon E, Legros C, Boutin JA, and Jockers R (2020) Journal of Pineal Research guideline for authors: Defining and characterizing melatonin targets. *J Pineal Res:*e12712 doi: 10.1111/jpi.12712.

Cheng Y and Prusoff WH (1973) Relationship between the inhibition constant (K1) and the concentration of inhibitor which causes 50 per cent inhibition (I50) of an enzymatic reaction. *Biochem Pharmacol* **22:**3099–3108 doi: 10.1016/0006-2952(73)90196-2.

Cogé F, Guenin SP, Fery I, Migaud M, Devavry S, Slugocki C, Legros C, Ouvry C, Cohen W, Renault N, Nosjean O, Malpaux B, Delagrange P, and Boutin JA (2009) The end of a myth: cloning and characterization of the ovine melatonin MT(2) receptor. *Br J Pharmacol* **158:**1248–1262 doi: 10.1111/j.1476-5381.2009.00453.x.

deReviers M-M, Ravault J-P, Tillet Y, and Pelletier J (1989) Melatonin binding sites in the sheep pars tuberalis. *Neuroscience letters* **100:**89–93 doi: 10.1016/0304-3940(89)90665-4.

Devavry S, Legros C, Brasseur C, Cohen W, Guenin S-P, Delagrange P, Malpaux B, Ouvry C, Cogé F, Nosjean O, and Boutin JA (2012) Molecular pharmacology of the mouse melatonin receptors MT_1 and MT_2. *Eur J Pharmacol* **677:**15–21 doi: 10.1016/j.ejphar.2011.12.009.

Dubocovich ML (1995) Melatonin receptors: Are there multiple subtypes? *Trends in Pharmacological Sciences* **16:**50–56 doi: 10.1016/S0165-6147(00)88978-6.

Duncan MJ, Takahashi JS, and Dubocovich ML (1986) Characterization of 2-[125I]iodomelatonin binding sites in hamster brain. *Eur J Pharmacol* **132:**333–334 doi: 10.1016/0014-2999(86)90627-8.

Ettaoussi M, Laversin A, Vreulz B, Rami M, Delagrange P, Caignard DH, Lebègue N, Melnyk P, Liberelle M, and Yous S (2021) Synthesis and SAR studies of Novel Isoquinoline and Tetrahydroisoquinoline Derivatives as Melatonin Receptor Ligands. *Eur. J. Med. Chem.*:submitted.

Gautier C, Dufour E, Dupré C, Lizzo G, Caignard S, Riest-Fery I, Brasseur C, Legros C, Delagrange P, Nosjean O, Simonneaux V, Boutin JA, and Guenin S-P (2018) Hamster Melatonin Receptors: Cloning and Binding Characterization of MT_1 and Attempt to Clone MT_2. *Int J Mol Sci* **19** doi: 10.3390/ijms19071957.

Harthé C, Claudy D, Déchaud H, Vivien-Roels B, Pévet P, and Claustrat B (2003) Radioimmunoassay of N-acetyl-N-formyl-5-methoxykynuramine (AFMK): a melatonin oxidative metabolite. *Life Sciences* **73:**1587–1597 doi: 10.1016/s0024-3205(03)00483-1.

Jacobs S, Chang K-J, and Cuatrecasas P (1975) Estimation of hormone receptor affinity by competitive displacement of labeled ligand: Effect of concentration of receptor and of labeled ligand. *Biochemical and Biophysical Research Communications* **66:**687–692 doi: 10.1016/0006-291X(75)90564-1.

Jan JE, Reiter RJ, Wong PKH, Bax MCO, Ribary U, and Wasdell MB (2011) Melatonin has membrane receptor-independent hypnotic action on neurons: an hypothesis. *J Pineal Res* **50:**233–240 doi: 10.1111/j.1600-079X.2010.00844.x.

Jockers R, Maurice P, Boutin JA, and Delagrange P (2008) Melatonin receptors, heterodimerization, signal transduction and binding sites: what's new? *Br J Pharmacol* **154:**1182–1195 doi: 10.1038/bjp.2008.184.

Johansson LC, Stauch B, McCorvy JD, Han GW, Patel N, Huang X-P, Batyuk A, Gati C, Slocum ST, Li C, Grandner JM, Hao S, Olsen RHJ, Tribo AR, Zaare S, Zhu L, Zatsepin NA, Weierstall U, Yous S, Stevens RC, Liu W, Roth BL, Katritch V, and Cherezov V (2019) XFEL structures of the human MT2 melatonin receptor reveal the basis of subtype selectivity. *Nature* **569:**289–292 doi: 10.1038/s41586-019-1144-0.

Kamal M, Gbahou F, Guillaume J-L, Daulat AM, Benleulmi-Chaachoua A, Luka M, Chen P, Kalbasi Anaraki D, Baroncini M, La Mannoury Cour C, Millan MJ, Prevot V, Delagrange P, and Jockers R (2015) Convergence of melatonin and serotonin (5-HT) signaling at MT2/5-HT2C receptor heteromers. *J Biol Chem* **290:**11537–11546 doi: 10.1074/jbc.M114.559542.

Leclerc V, Fourmaintraux E, Depreux P, Lesieur D, Morgan P, Howell H, Renard P, Caignard D-H, Pfeiffer B, Delagrange P, Guardiola-Lemaître B, and Andrieux J (1998) Synthesis and structure–activity relationships of novel naphthalenic and bioisosteric related amidic derivatives as melatonin receptor ligands. *Bioorganic & medicinal chemistry* **6:**1875–1887 doi: 10.1016/s0968-0896(98)00147-3.

Leclerc V, Yous S, Delagrange P, Boutin JA, Renard P, and Lesieur D (2002) Synthesis of nitroindole derivatives with high affinity and selectivity for melatoninergic binding sites MT(3). *J Med Chem* **45:**1853–1859 doi: 10.1021/jm011053.

Legros C, Chesneau D, Boutin JA, Barc C, and Malpaux B (2014a) Melatonin from cerebrospinal fluid but not from blood reaches sheep cerebral tissues under physiological conditions. *J Neuroendocrinol* **26:**151–163 doi: 10.1111/jne.12134.

Legros C, Devavry S, Caignard S, Tessier C, Delagrange P, Ouvry C, Boutin JA, and Nosjean O (2014b) Melatonin MT_1 and MT_2 receptors display different molecular pharmacologies only in the G-protein coupled state. *Br J Pharmacol* **171:**186–201 doi: 10.1111/bph.12457.

Legros C, Dupré C, Brasseur C, Bonnaud A, Bruno O, Valour D, Shabajee P, Giganti A, Nosjean O, Kenakin TP, and Boutin JA (2020) Characterization of the various functional pathways elicited by

synthetic agonists or antagonists at the melatonin MT1 and MT2 receptors. *Pharmacol Res Perspect* **8:**e00539 doi: 10.1002/prp2.539.

Legros C, Matthey U, Grelak T, Pedragona-Moreau S, Hassler W, Yous S, Thomas E, Suzenet F, Folleas B, Lefoulon F, Berthelot P, Caignard D-H, Guillaumet G, Delagrange P, Brayer J-L, Nosjean O, and Boutin JA (2013) New radioligands for describing the molecular pharmacology of MT1 and MT2 melatonin receptors. *Int J Mol Sci* **14:**8948–8962 doi: 10.3390/ijms14058948.

Liu L, Labani N, Cecon E, and Jockers R (2019) Melatonin Target Proteins: Too Many or Not Enough? *Front Endocrinol (Lausanne)* **10:**791 doi: 10.3389/fendo.2019.00791.

Lozinskaya N, Sosonyuk S, Volkova M, Seliverstov M, Proskurnina M, Bachurin S, and Zefirov N (2011) Simple Synthesis of Some 2-Substituted Melatonin Derivatives. *Synthesis* **2011:**273–276 doi: 10.1055/s-0030-1258361.

Mailliet F, Audinot V, Malpaux B, Bonnaud A, Delagrange P, Migaud M, Barrett P, Viaud-Massuard M-C, Lesieur D, Lefoulon F, Renard P, and Boutin JA (2004) Molecular pharmacology of the ovine melatonin receptor: comparison with recombinant human MT1 and MT2 receptors. *Biochem Pharmacol* **67:**667–677 doi: 10.1016/j.bcp.2003.09.037.

Malpaux B, Daveau A, Maurice-Mandon F, Duarte G, and Chemineau P (1998) Evidence that melatonin acts in the premammillary hypothalamic area to control reproduction in the ewe: presence of binding sites and stimulation of luteinizing hormone secretion by in situ microimplant delivery. *Endocrinology* **139:**1508–1516 doi: 10.1210/endo.139.4.5879.

Migaud M, Daveau A, and Malpaux B (2005) MTNR1A melatonin receptors in the ovine premammillary hypothalamus: day-night variation in the expression of the transcripts. *Biol Reprod* **72:**393–398 doi: 10.1095/biolreprod.104.030064.

Morgan PJ, Williams LM, Davidson G, Lawson W, and Howell E (1989) Melatonin receptors on ovine pars tuberalis: characterization and autoradiographicai localization. *J Neuroendocrinol* **1:**1–4 doi: 10.1111/j.1365-2826.1989.tb00068.x.

Nosjean O, Ferro M, Coge F, Beauverger P, Henlin JM, Lefoulon F, Fauchere JL, Delagrange P, Canet E, and Boutin JA (2000) Identification of the melatonin-binding site MT3 as the quinone reductase 2. *J Biol Chem* **275:**31311–31317 doi: 10.1074/jbc.M005141200.

Nosjean O, Nicolas JP, Klupsch F, Delagrange P, Canet E, and Boutin JA (2001) Comparative pharmacological studies of melatonin receptors: MT1, MT2 and MT3/QR2. Tissue distribution of MT3/QR2. *Biochem Pharmacol* **61:**1369–1379 doi: 10.1016/s0006-2952(01)00615-3.

Pandi-Perumal SR, Srinivasan V, Maestroni GJM, Cardinali DP, Poeggeler B, and Hardeland R (2006) Melatonin: Nature's most versatile biological signal? *FEBS J* **273:**2813–2838 doi: 10.1111/j.1742-4658.2006.05322.x.

Piketty V and Pelletier J (1993) Melatonin receptors in the lamb pars tuberalis/median eminence throughout the day. *Neuroendocrinology* **58:**359–365 doi: 10.1159/000126563.

Reppert SM, Godson C, Mahle CD, Weaver DR, Slaugenhaupt SA, and Gusella JF (1995) Molecular characterization of a second melatonin receptor expressed in human retina and brain: the Mel1b melatonin receptor. *Proc Natl Acad Sci U S A* **92:**8734–8738 doi: 10.1073/pnas.92.19.8734.

Reppert SM, Weaver DR, and Ebisawa T (1994) Cloning and characterization of a mammalian melatonin receptor that mediates reproductive and circadian responses. *Neuron* **13:**1177–1185 doi: 10.1016/0896-6273(94)90055-8.

Stankov B, Cozzi B, Lucini V, Fumagalli P, Scaglione F, and Fraschini F (1991) Characterization and mapping of melatonin receptors in the brain of three mammalian species: rabbit, horse and sheep. A comparative in vitro binding study. *Neuroendocrinology* **53:**214–221 doi: 10.1159/000125721.

Stauch B, Johansson LC, McCorvy JD, Patel N, Han GW, Huang X-P, Gati C, Batyuk A, Slocum ST, Ishchenko A, Brehm W, White TA, Michaelian N, Madsen C, Zhu L, Grant TD, Grandner JM, Shiriaeva A, Olsen RHJ, Tribo AR, Yous S, Stevens RC, Weierstall U, Katritch V, Roth BL, Liu W, and Cherezov V (2019) Structural basis of ligand recognition at the human MT1 melatonin receptor. *Nature* **569:**284–288 doi: 10.1038/s41586-019-1141-3.

Suofu Y, Li W, Jean-Alphonse FG, Jia J, Khattar NK, Li J, Baranov SV, Leronni D, Mihalik AC, He Y, Cecon E, Wehbi VL, Kim J, Heath BE, Baranova OV, Wang X, Gable MJ, Kretz ES, Di Benedetto G, Lezon TR, Ferrando LM, Larkin TM, Sullivan M, Yablonska S, Wang J, Minnigh MB, Guillaumet G, Suzenet F, Richardson RM, Poloyac SM, Stolz DB, Jockers R, Witt-Enderby PA, Carlisle DL, Vilardaga J-P, and Friedlander RM (2017) Dual role of mitochondria in producing melatonin and driving GPCR signaling to block cytochrome c release. *Proc Natl Acad Sci U S A* **114:**E7997-E8006 doi: 10.1073/pnas.1705768114.

Zhen J, Antonio T, Dutta AK, and Reith MEA (2010) Concentration of receptor and ligand revisited in a modified receptor binding protocol for high-affinity radioligands: 3HSpiperone binding to D2 and D3 dopamine receptors. *J Neurosci Methods* **188:**32–38 doi: 10.1016/j.jneumeth.2010.01.031.

JPET Fast Forward. Published on October 27, 2021 as DOI: 10.1124/jpet.121.000785
This article has not been copyedited and formatted. The final version may differ from this version.

Footnotes:

This work was not supported by external funding.

[1] Jean A. Boutin present address: PHARMADEV (Pharmacochimie et biologie pour le développement), Faculté de Pharmacie, Toulouse, France.

[2] Céline Legros present address: Eurofins Discovery, Eurofins Cerep, Le Bois L'évêque, Celle-l'Evescault, France.

JPET Fast Forward. Published on October 27, 2021 as DOI: 10.1124/jpet.121.000785
This article has not been copyedited and formatted. The final version may differ from this version.

Legends to the figures

Scheme 1: **Schematic representation of the areas used for hypothalamic membranes.**

Sheep brain was dissected at 4°C as a piece of tissue centered on the premammillary hypothalamus (PMH) area, laterally limited by column of the fornix (Fx) and the mammillothalamic tract (MT), ventrally by the base of the brain and dorsally by the floor of the lateral ventricle (LV).

Figure 1: Structures of the melatoninergic compounds used in the experiments.

MLT, melatonin; 2-I-MLT, 2-iodo-melatonin; S 22153, N-[2-(5-ethylbenzothiophen-3-yl)ethyl]acetamide; 4P-PDOT, 4-phenyl-2-propionamidotetraline; MCA-NAT, 5-methoxy-carbonylamino-N-acetyltryptamine; SD 1882, 4-iodo-melatonin; SD 1918, 7-iodo-melatonin; S 27128, 2-iodo-6-nitro-melatonin; S 22958, 4-(8-chloro-7-methoxy-1-naphthyl)-N-ethyl-butanamide; S 73229, N-[2-(5-methoxy-2-oxo-indolin-3(RS)-yl)ethyl]acetamide, racemate; S 70643, N-[2-(6-methoxy-4-isoquinolyl)ethyl]acetamide, hydrogen chloride; NAS, N-acetyl-serotonin; SD 1671, N-[3-(2-amino-5-methoxy-phenyl)-3-oxo-propyl]acetamide.

Figure 2: Distribution and quantification of the binding pattern autoradiography in sheep brain.

Distribution and quantification of the 2-[^{125}I]-MLT binding patterns in hypothalamic areas and *pars tuberalis* of the sheep brain. Left panel: Pseudo-colored representative autoradiographs obtained at 4 different concentrations of 2-[^{125}I]-MLT in the absence (left column) and in the presence (right column) of 10 µM MLT. The color code refers to binding intensity. Right Panel: Quantification of total (blue bars) and non-specific (red bars) binding in brain regions of interest for increasing concentrations of 2-[^{125}I]-MLT. Mean ± SD, 2 animals, at least 4 autoradiography slices per animal per structure per concentration. (**A**): *Pars tuberalis*; (**B**): Sub-fornical space; (**C**): 3rd ventricle; (**D**): Lateral ventricle. The two different exposure times were due to the rapid saturation of the *pars tuberalis* autoradiography, due to the presence in this tissue of the classical MLT receptors.

JPET Fast Forward. Published on October 27, 2021 as DOI: 10.1124/jpet.121.000785
This article has not been copyedited and formatted. The final version may differ from this version.

Figure 3: Melatonin binding sites in *pars tuberalis* of sheep brain.

A: Evolution of the density of specific MLT binding site (oMT_1/oMT_2) on the *pars tuberalis* in function of the concentration of 2-[^{125}I]-MLT.

B: Saturation curve and corresponding linear regression of specific 2-[^{125}I]-MLT binding to *pars tuberalis* membranes (n = 4). In *pars tuberalis*, only oMT_1 receptor is present and saturation is reached for concentrations higher than 270 pM.

Figure 4: Melatonin binding sites in the sheep brain.

Evolution of density of specific MLT binding site on different areas of the hypothalamus in function of the concentration of the 2-[^{125}I]-MLT from autoradiography. Each color matches with an area of interest and to a histogram bar as depicted on the brain scheme in the upper panel. In the hypothalamus (blue histograms), a first plateau is obtained for concentrations between 270 and 3200 pM (saturation of oMT_1 receptor). For higher concentrations, the specific binding increases, showing a new low affinity binding site.

Blue: *Pars tuberalis*; Pink: sub-fornical space/premammillary hypothalamus; Green: border of the third ventricle; Orange: border of the lateral ventricle (LV); Purple: mid region between lateral ventricle and third ventricle (3rdV); Yellow: mammillothalamic tract (MT).

Figure 5: Melatonin binding sites in the *pars tuberalis* of sheep brain.

Saturation curve and corresponding linear regressions (two sites model statistically determined in saturation analysis) of specific 2-[^{125}I]-MLT binding to hypothalamic membranes (n = 17). In hypothalamus, a second low affinity binding site is present, in addition to the oMT_1 receptor.

Figure 6: Pharmacological profile of the putative binding site, MTx.

JPET Fast Forward. Published on October 27, 2021 as DOI: 10.1124/jpet.121.000785
This article has not been copyedited and formatted. The final version may differ from this version.

Dose-displacement curves for inhibition of 2-[^{125}I]-MLT binding to hypothalamic membranes by various melatoninergic and serotoninergic ligands. Hypothalamic membranes were incubated 4 h at room temperature with 35 pM (circles) or 350 pM (triangles) of 2-[^{125}I]-MLT. The data are plotted as the percentage of specific 2-[^{125}I]-MLT bound vs. the concentration of competing drug. Each curve represents the mean ± S.E.M. of 2 (35 pM) or 4 (350 pM) independent experiments, in triplicate. From top to bottom, from left to right: 2-iodo-MLT, MLT, SD 1882, S 27128, 4P-PDOT, MCA-NAT, Ketanserine, 5-HT, NAS and S 22153.

Figure 7: Saturation curves and linear regression for MTx in hypothalamus membranes.

Specific 2-[^{125}I]-MLT binding was performed with hypothalamic membranes in the absence (**A**) or in the presence of 1 pM of SD 1882 (**B**, n = 3) or S 27128 (**C,** n = 3). In hypothalamus, addition of SD 1882 or S 27128 induced the disappearance of the low affinity binding site without changing oMT_1 characteristics, as can be seen by comparing with binding curve from *pars tuberalis* membranes (**D**).

Figure 8: Differential pharmacological profile of the putative binding site, MTx.

Dose-displacement curves for inhibition of 2-[^{125}I]-MLT binding to hypothalamic membranes by 2-I-MLT (**A**) and MLT (**B**) in absence (**A,D**) or in presence (**B**,**C**) of 1 pM SD 1882 and S 27128 or 1 µM S 22153. Hypothalamic membranes were incubated 4 h at room temperature with 350 pM of 2-[^{125}I]-MLT. The data are plotted as the percentage of specific 2-[^{125}I]-MLT bound versus the concentration of competing drug. Each curve represents the mean ± S.E.M. of 3 independent experiments, in triplicate.

Panel B: squares: 2-I-MLT + SD 1882; circles: 2-I-MLT + S 27128; diamonds: 2-I-MLT + S 22153.

Panel C: squares: MLT + SD 1882; circles: MLT + S 27128; diamonds: MLT + S 22153.

Figure 9: Saturation curves and linear regression for MTx in sheep retina.

JPET Fast Forward. Published on October 27, 2021 as DOI: 10.1124/jpet.121.000785
This article has not been copyedited and formatted. The final version may differ from this version.

Saturation curve and corresponding Scatchard plot of specific 2-[^{125}I]-MLT binding to retina membranes (n = 5). In retina, a second low affinity binding site (pK_D = 8.81 ± 0.5, Bmax = 7.65 ± 2.64 fmol/mg protein) is present, in addition to the oMT1 receptor (pK_D = 10.18 ± 0.20, Bmax = 2.47 ± 0.43 fmol/mg protein).

JPET Fast Forward. Published on October 27, 2021 as DOI: 10.1124/jpet.121.000785
This article has not been copyedited and formatted. The final version may differ from this version.

Table 1: Data summary from the saturation curves of *pars tuberalis* and hypothalamic membranes in control conditions and of hypothalamus in the presence of 1 pM SD 1882 or S 27128.

	oMT_1/oMT_2		**MTx**	
	pK_D	**Bmax (fmol/mg)**	**pK_D**	**Bmax (fmol/mg)**
***Pars tuberalis* (n = 4)**	10.88 ± 0.07	39.5 ± 8.0	-	-
Hypothalamus (n = 17)	10.58 ± 0.07	0.40 ± 0.05	9.13 ± 0.05	1.12 ± 0.11
Hypothalamus + SD 1882 (n = 3)	10.49 ± 0.20	0.59 ± 0.15	-	-
Hypothalamus + S 27128 (n = 3)	10.51 ± 0.19	0.60 ± 0.13	-	-

JPET Fast Forward. Published on October 27, 2021 as DOI: 10.1124/jpet.121.000785
This article has not been copyedited and formatted. The final version may differ from this version.

Table 2: Binding affinities at oMT_1/oMT_2 receptor and MTx binding site in *pars tuberalis* and hypothalamus membranes.

	35 pM 2-[^{125}I]-MLT		350 pM 2-[^{125}I]-MLT	
	Pars tuberalis	Hypothalamus	Hypothalamus	
	pK_i oMT_1/oMT_2		pK_i oMT_1/oMT_2	pK_i MTx (pM)[a]
MLT	10.38 ± 0.08	9.76 ± 0.07	9.77 ± 0.11	13.08 ± 0.18
2-I-MLT	10.46 ± 0.04	10.41 ± 0.06	10.61 ± 0.09	13.24 ± 0.14
S 22153	8.16 ± 0.26	7.84 ± 0.10	7.39 ± 0.30	-
4P-PDOT	7.13 ± 0.17	6.59 ± 0.56	6.39	13.27 ± 0.31[a]
MCA-NAT	-	-	-	-
SD 1882	8.51 ± 0.04	7.65 ± 0.14	7.87 ± 0.44	12.78 ± 0.37
SD 1918	7.80 ± 0.09	7.57 ± 0.37	7.16 ± 0.55	12.64 ± 0.36
S 27128	9.07 ± 0.13	9.46 ± 0.09	9.34 ± 0.27	12.86 ± 0.39[a]
S 22958	8.25 ± 0.10	8.07 ± 0.30	8.12 ± 0.63	13.76 ± 0.26[a]
S 73229	6.84 ± 0.26	6.91 ± 0.20	-	13.52 ± 0.19[a]
S 70643	8.62 ± 0.14	8.19 ± 0.02	7.33 ± 0.36	13.52 ± 0.09[a]
5-HT	-	-	-	14.08 ± 0.52[a]
NAS	7.30 ± 0.08	6.34± 0.41	-	13.55 ± 0.23[a]
SD 1671	7.73 ± 0.17	7.57 ± 0.09	-	13.66 ± 0.29[a]
DOI	-	-	-	-
Ketanserine	-	-	-	-
DA	-	-	-	-
NA	-	-	-	-

Binding affinities are expressed as mean pK_i ± S.E.M. of at least 2 independent experiments for *pars tuberalis* and hypothalamus at 35 pM of 2-[^{125}I]-MLT and 4 independent experiments for hypothalamus at 350 pM of 2-[^{125}I]-MLT, in triplicate. [a]pIC_{50} values instead, as indicated. (-) indicates no affinity of the molecule for MLT binding site(s).

JPET Fast Forward. Published on October 27, 2021 as DOI: 10.1124/jpet.121.000785
This article has not been copyedited and formatted. The final version may differ from this version.

Table 3: Data summary of competition curves on hypothalamic membranes for the MLT and 2-I-MLT in control conditions or in presence of 1 pM of SD 1882 and S 27128 or 1 µM of S 22153.

	pK_i MTx (pM)	**pK_i oMT_1/oMT_2 (pM)**
2-I-MLT	13.24 ± 0.14	10.61 ± 0.09
2-I-MLT + 1 pM SD 1882	-	10.42 ± 0.45
2-I-MLT + 1 pM S 27128	-	10.44 ± 0.50
2-I-MLT + 1 µM S 22153	13.15 ± 0.15	-
MLT	13.08 ± 0.18	9.77 ± 0.11
MLT + 1 pM SD 1882	-	9.80 ± 0.46
MLT + 1 pM S 27128	-	10.24 ± 0.79
MLT + 1 µM S 22153	13.15 ± 0.40	-

Binding affinities are expressed as mean pKi ± S.E.M. of at least 3 independent experiments at 350 pM of 2-[^{125}I]-MLT, in triplicate. (-) indicates no affinity of the molecule for MLT binding sites.

JPET Fast Forward. Published on October 27, 2021 as DOI: 10.1124/jpet.121.000785
This article has not been copyedited and formatted. The final version may differ from this version.

Table 4: Summary of the characteristics of the oMT_1/oMT_2 and the putative new MLT binding site, MTx, from sheep hypothalamus.

	oMT_1/oMT_2	MTx
Cellular localisation	**Plasma membranes** **Mitochondrial membranes**[a]	**Membranes**
Tissue expression	***Pars tuberalis*** **PMH** **Retina**	**PMH** **Retina**
Ligands	**MLT** $pK_i = 9.77 \pm 0.11$ **2-[^{125}I]-MLT** $pK_i = 10.61 \pm 0.09$ **S 22153** $pK_i = 7.39 \pm 0.30$	**MLT** $pK_i = 13.08 \pm 0.18$ **2-[^{125}I]-MLT** $pK_i = 13.24 \pm 0.14$ **5-HT** $pK_i = 14.08 \pm 0.52$ **SD 1882** $pK_i = 12.78 \pm 0.37$ **S 27128** $pK_i = 12.86 \pm 0.39$
Identification methods	**Autoradiography**	**Autoradiography**
Dimerization	**MT_2: pharmacological profile unchanged** **5-HT_{2c}: pharmacological profile unchanged**	**Unknown**

[a] (Suofu et al., 2017).

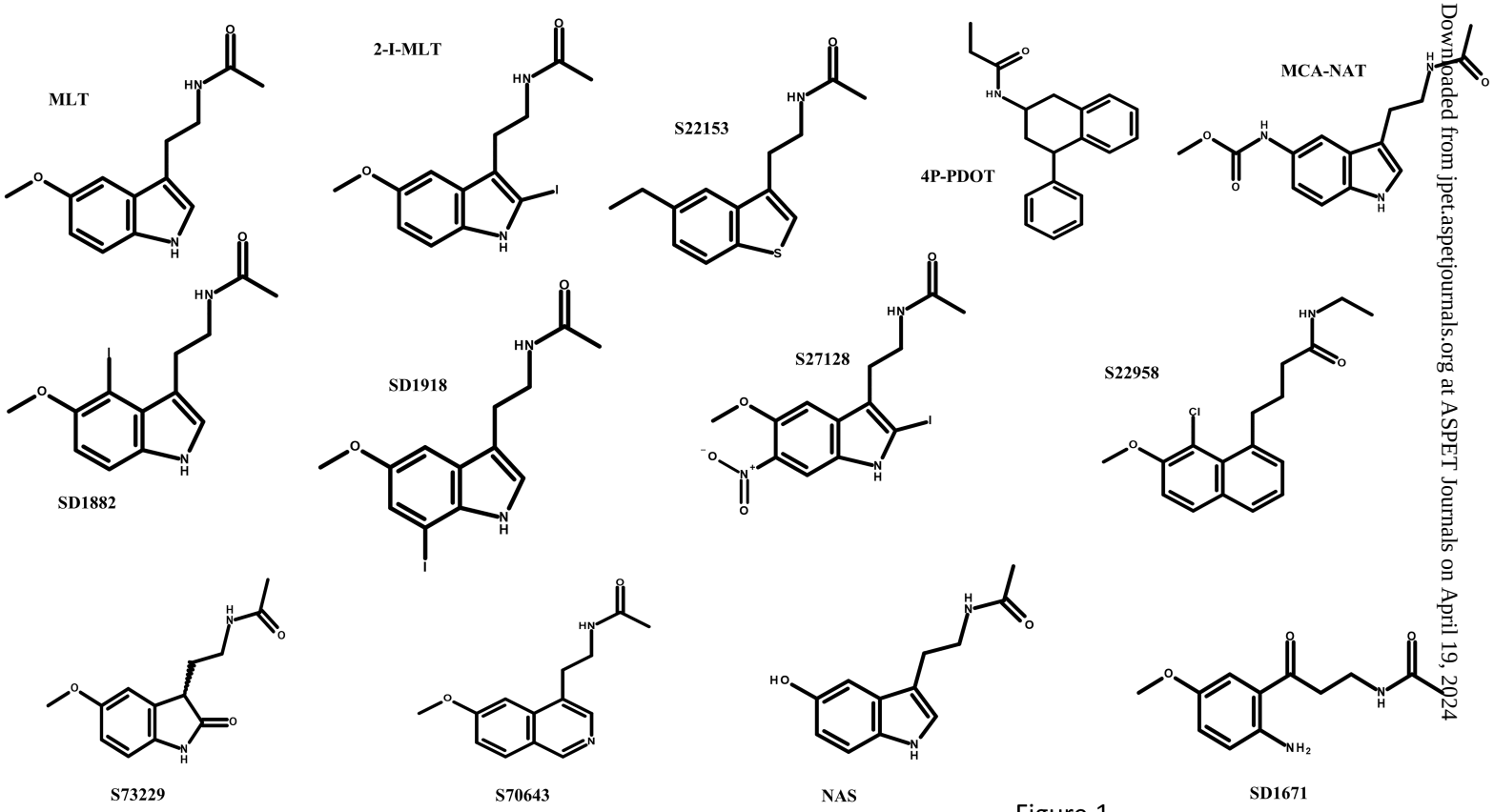

Figure 1

Figure 2

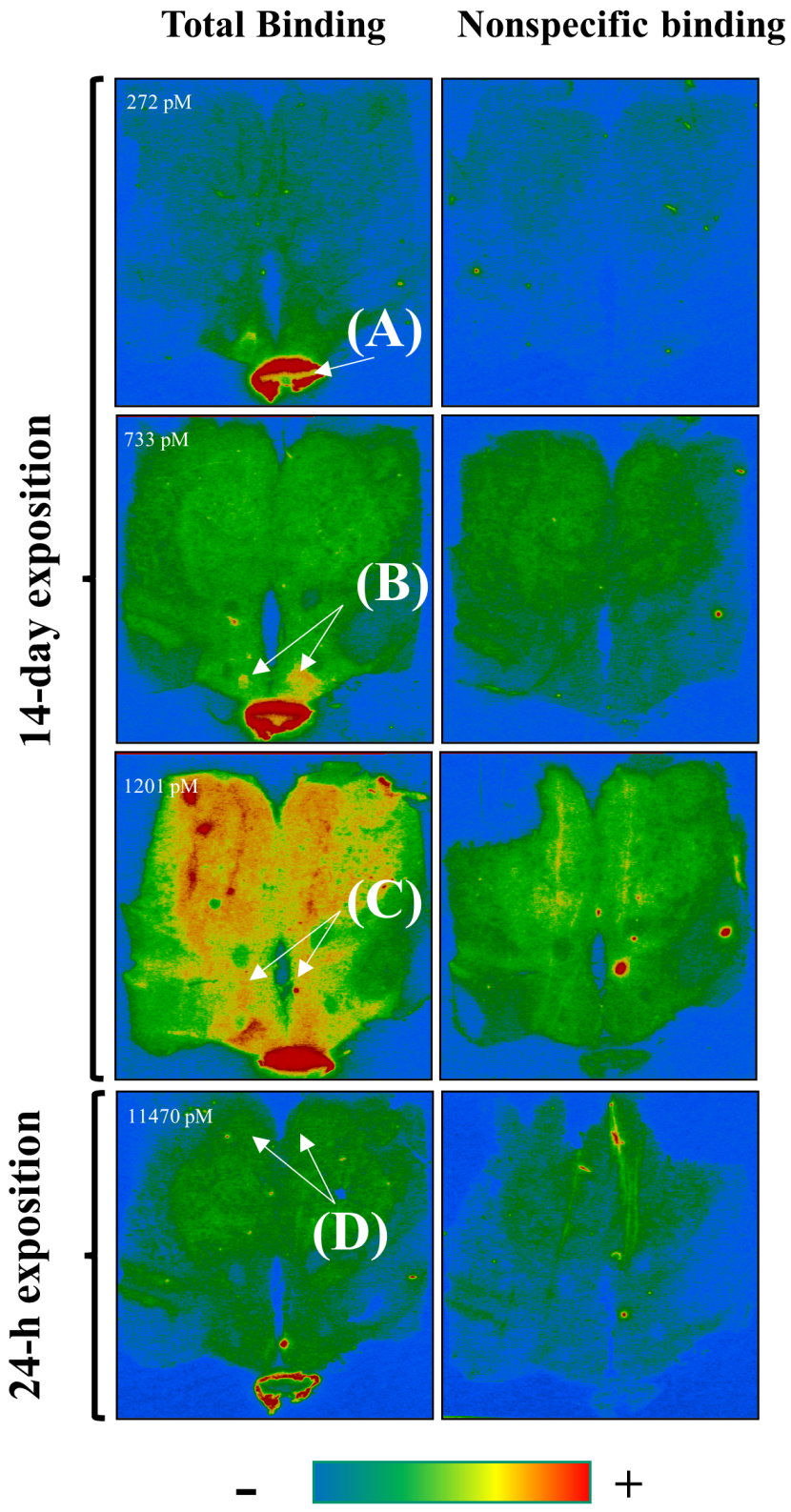

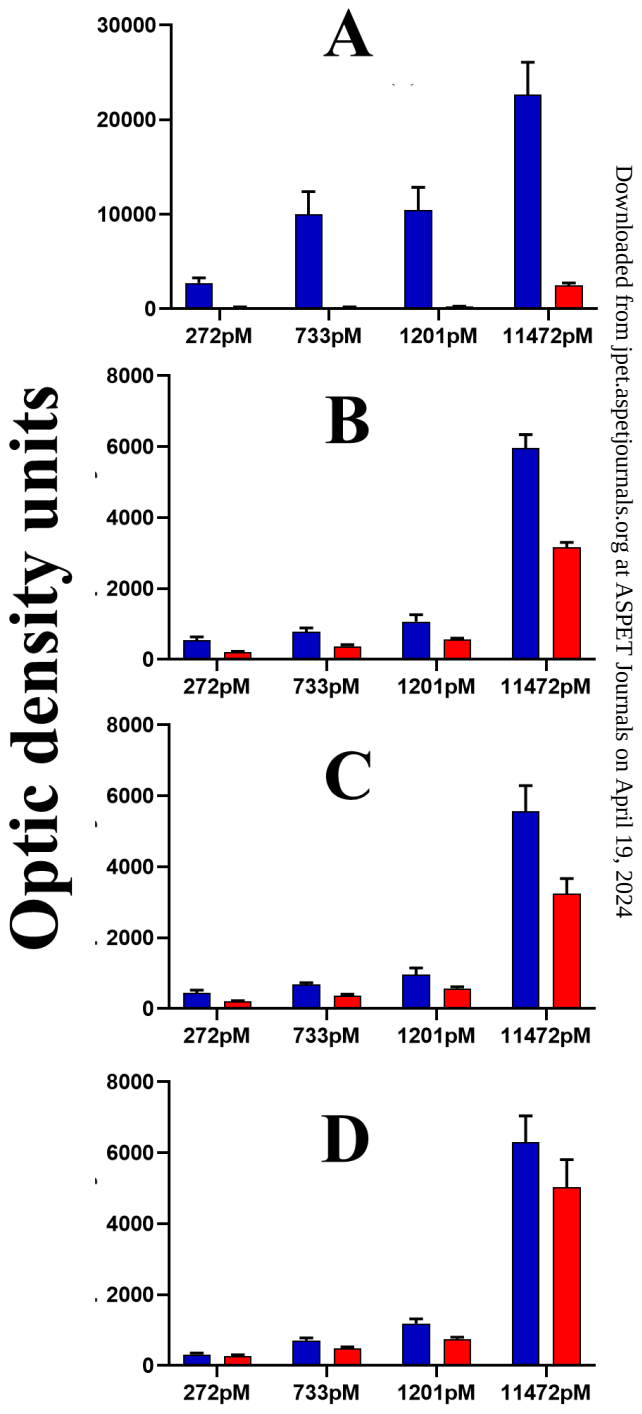

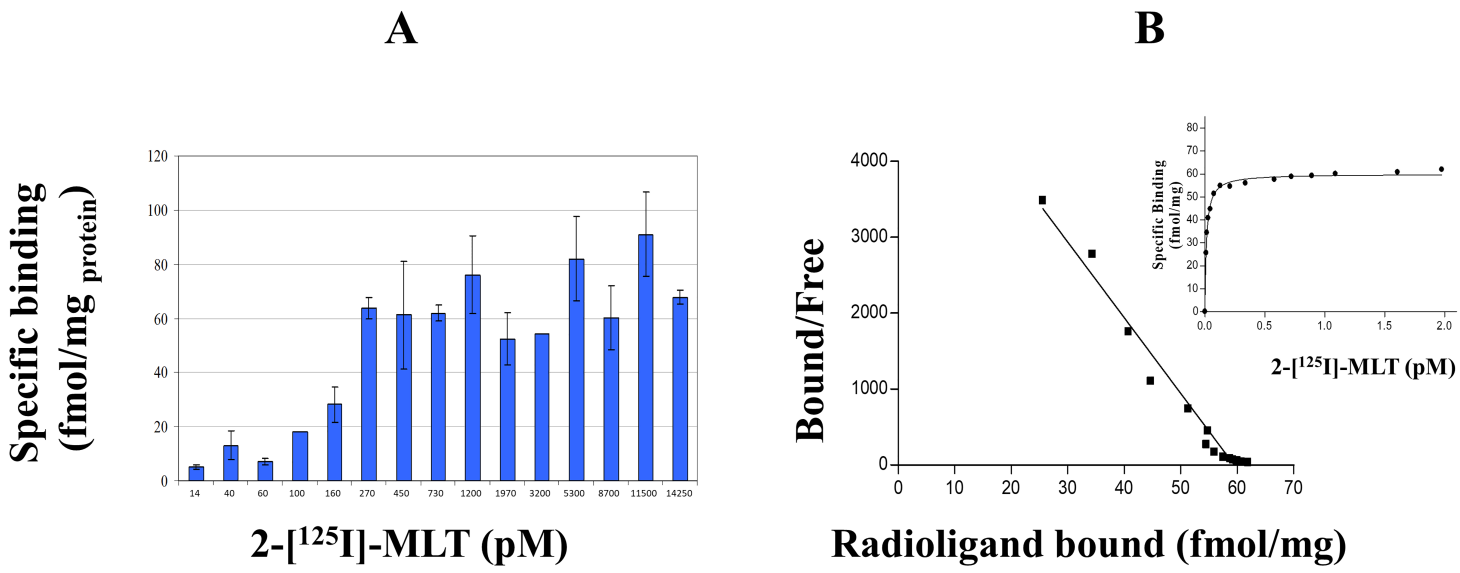

Figure 3

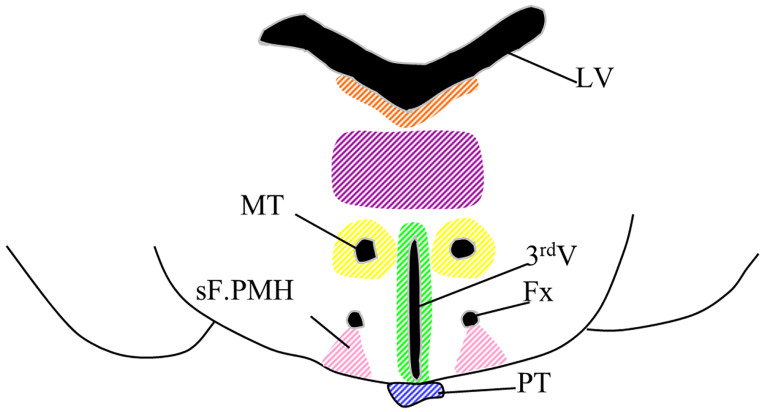

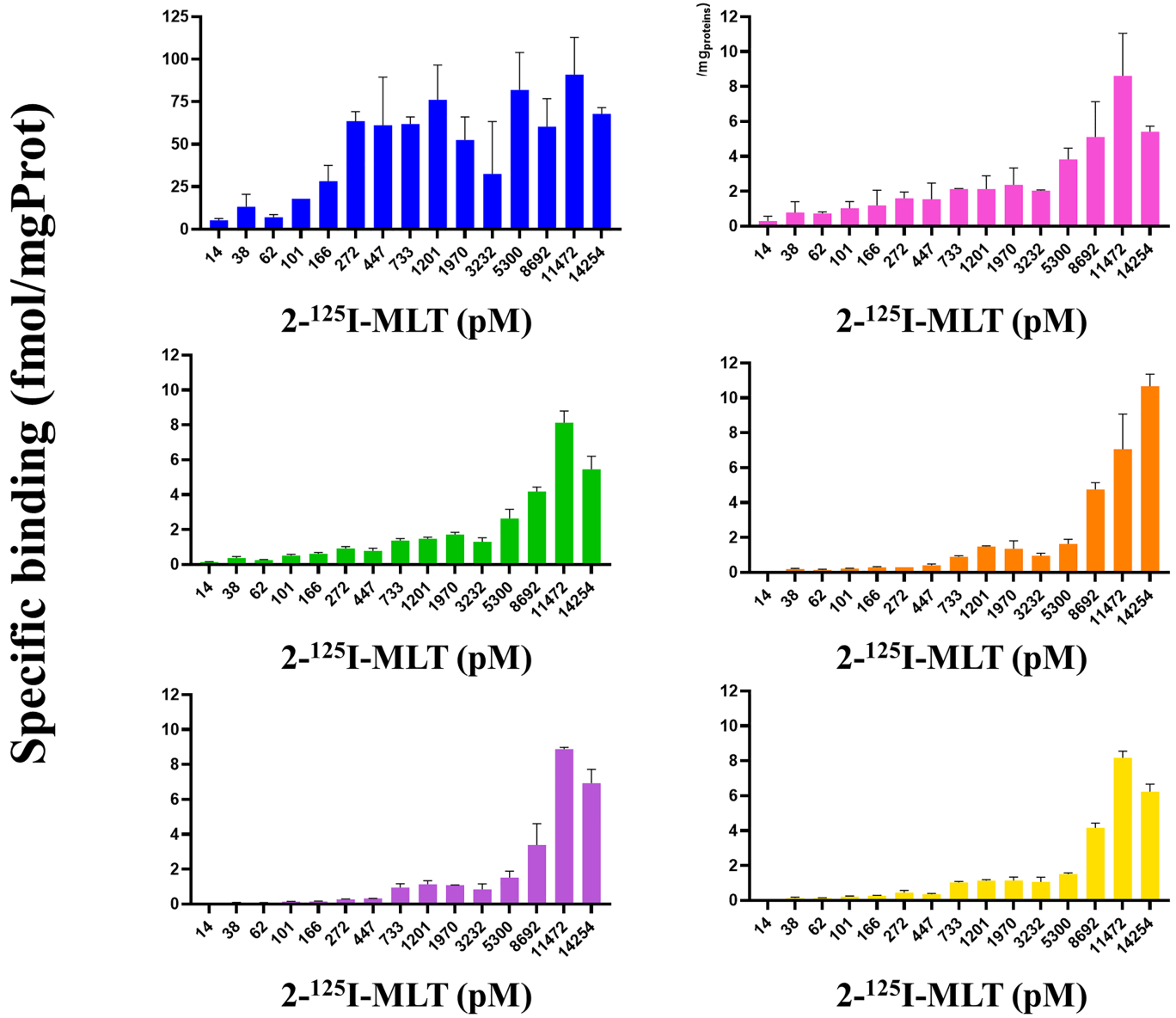

Figure 4

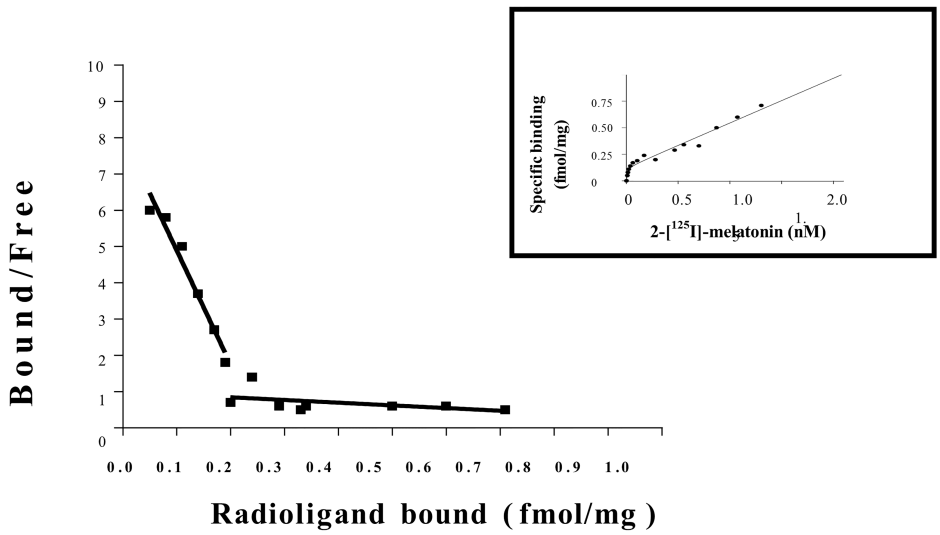

Figure 5

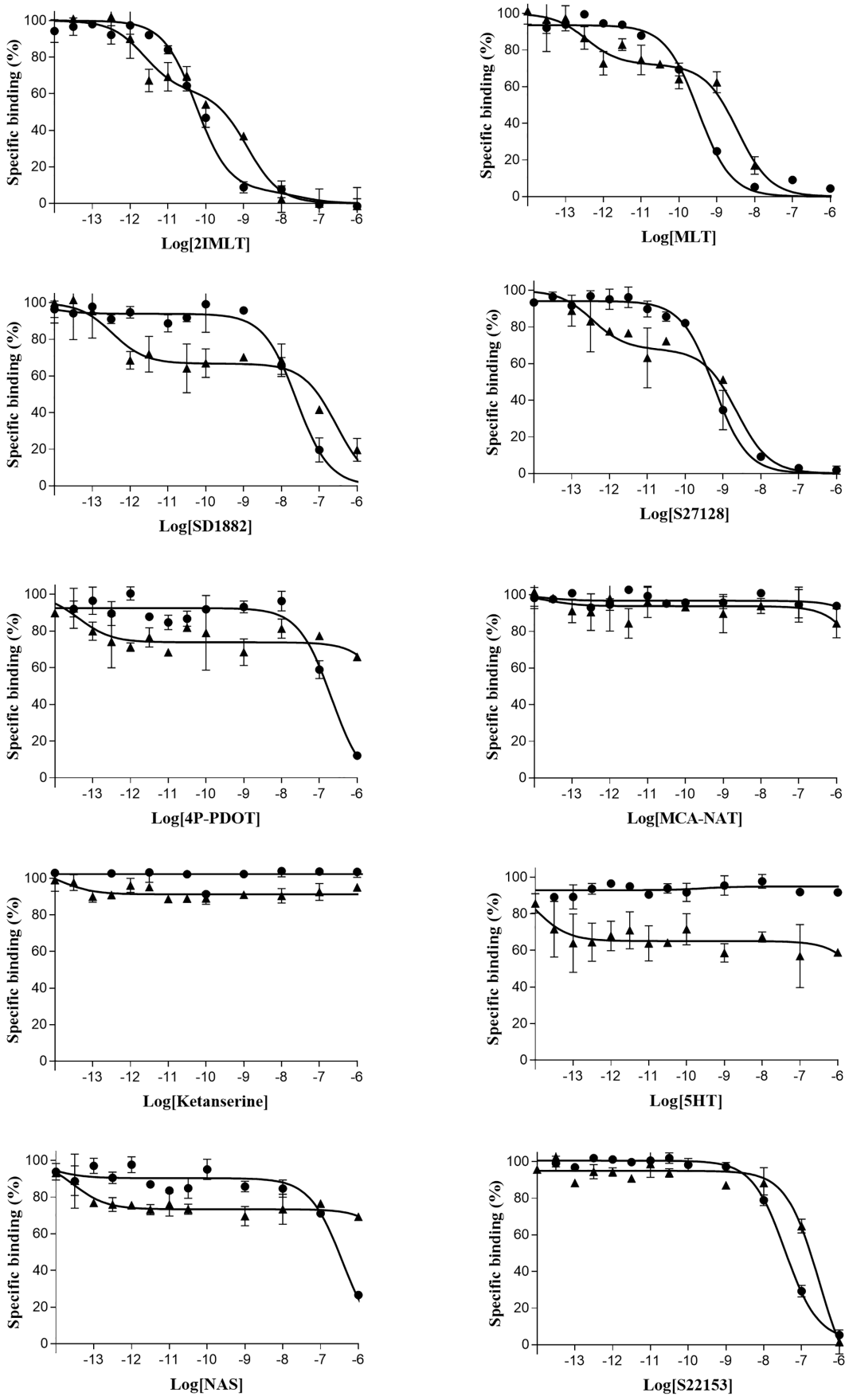

Figure 6

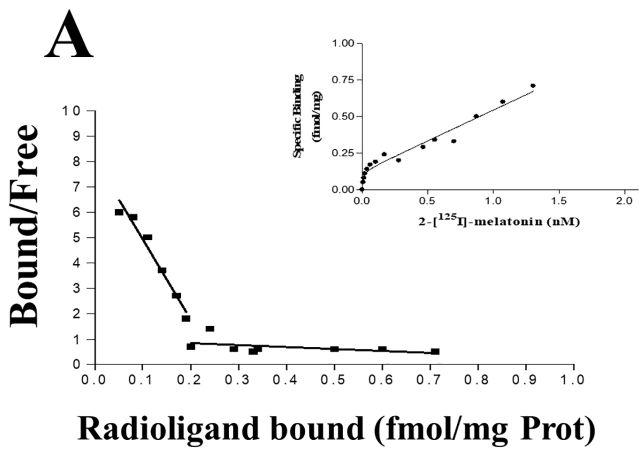

Hypothalamus

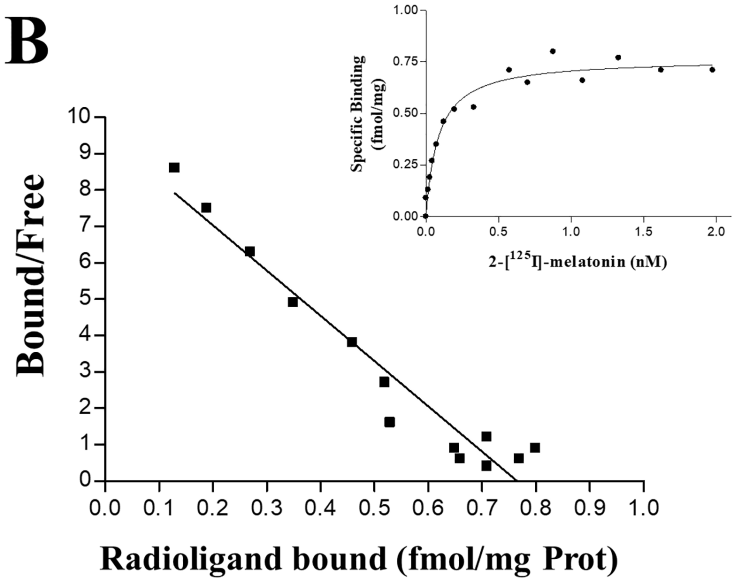

Hypothalamus + SD 1882 (1pM)

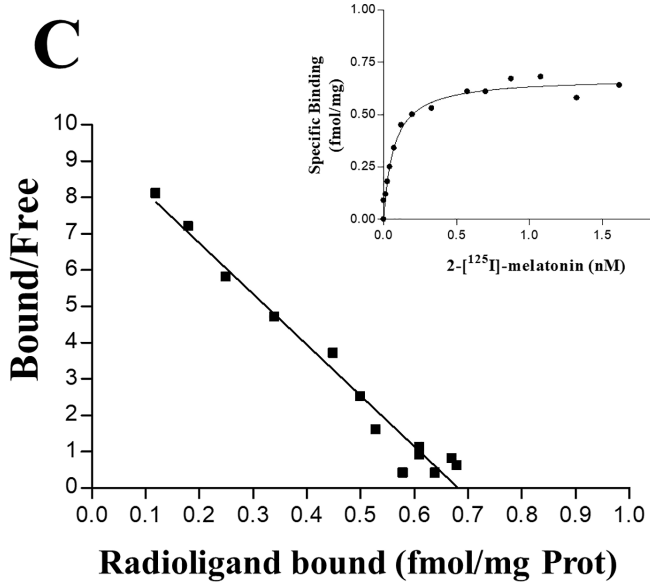

Hypothalamus + S 27128 (1pM)

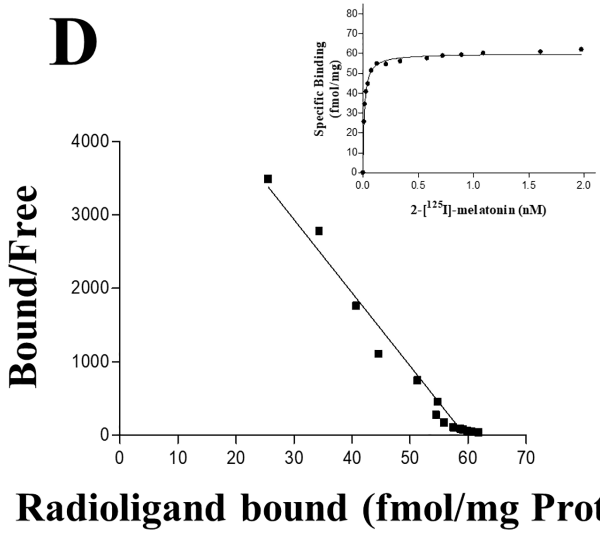

Pars tuberalis

Figure 7

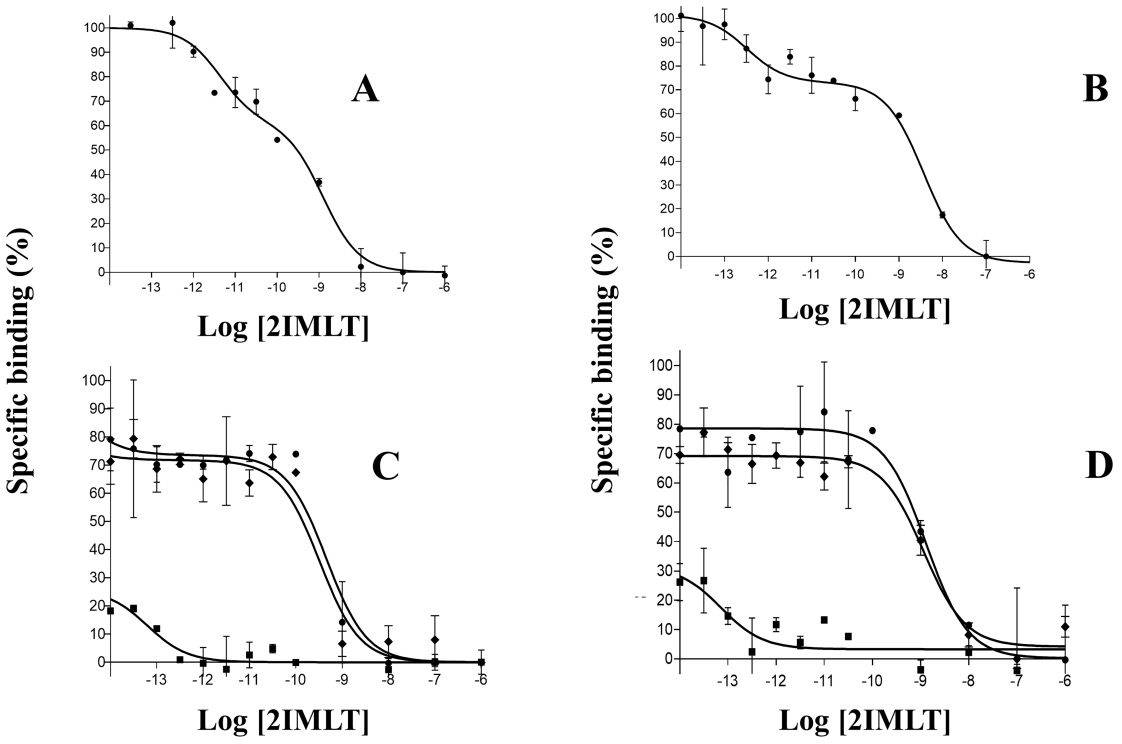

Figure 8

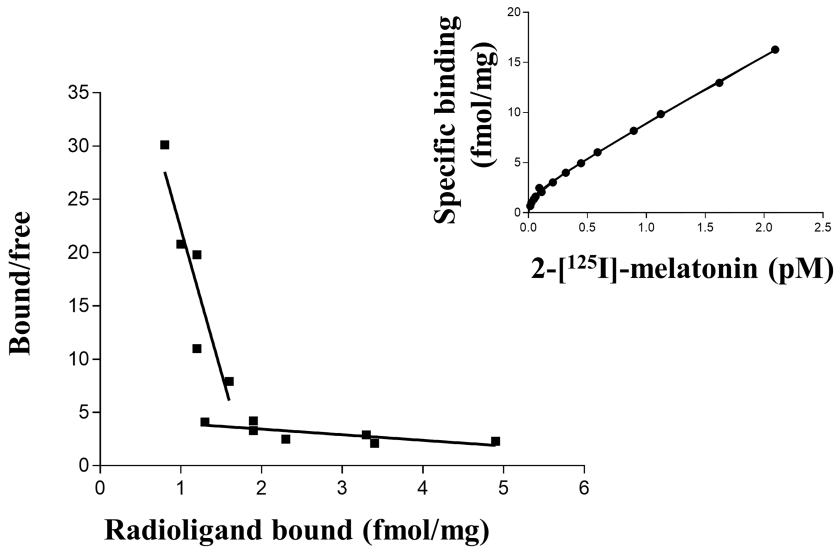

Figure 9

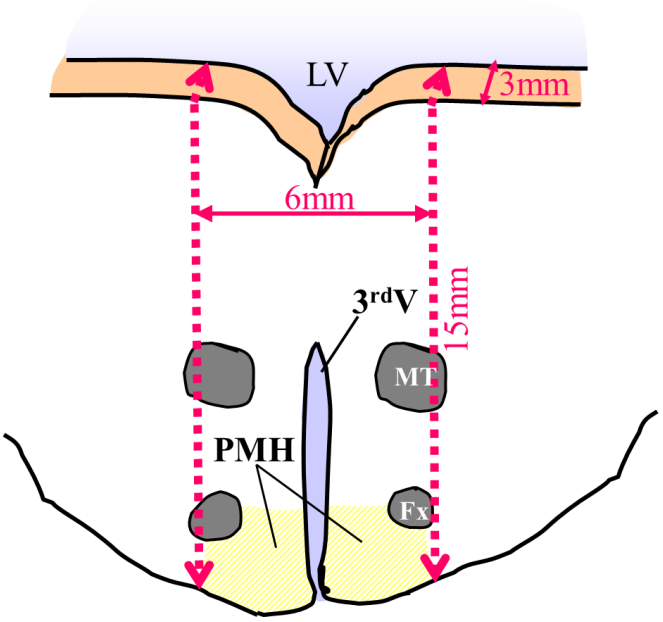

Scheme 1